NUMERICAL SIMULATIONS FOR TSUNAMI FORECASTING AT PADANG CITY USING OFFSHORE TSUNAMI SENSORS

Setyoajie Prayoedhie* **Supervisor: Yushiro FUJII****
MEE10518 **Bunichiro SHIBAZAKI****

ABSTRACT

We conducted numerical simulations to forecast near-field tsunami at ocean bottom tsunami meter (OBTM) and GPS buoy stations along the Sumatra Island. We used modeling codes of TUNAMI-N2 (Tohoku University's Numerical Analysis Model for Investigation of Near-Field Tsunami, No.2) and TUNAMI-F1(Far-Field Tsunami, No.1) developed by the Disaster Control Research Center (DCRC), Tohoku University, Japan in order to estimate the tsunami height and arrival time using proposed scenarios. For numerical simulation, we used three different scenario earthquakes which are considered along the Sunda trench. The source parameters for scenario earthquakes are based on the coral-reef study by Natawidjaja et al. (2006) for the earthquakes of 1797 (Mw 8.7) and 1833 (Mw 8.6 and 8.9). For the 1797 event (scenario 2), we obtained the tsunami height of 1.547 m with the arrival time of 0.8 min at TM2 offshore output point located in the uplift area, while 0.109 m and 3.9 min for the tsunami height and arrival time, respectively, at TM3 offshore output point located to the south from the source. Based on a simulation result for three scenarios using different bathymetry data (1 arc-minute and 30 arc-second), we found that the tsunami waves reach the coastal area in less than 40 min for the output point located in Padang city (OP2). By using detailed bathymetry data, we can estimate more accurate on tsunami arrival time and tsunami height.

Keywords: Tsunami forecasting, offshore tsunami sensor, scenario earthquakes, numerical simulation, Padang city.

1. INTRODUCTION

Since late 2004, a series of earthquakes, has ruptured the plate boundary from the Andaman Islands to the Sunda Strait, for a distance of nearly 2,500 km. Only 300-km long of the Sunda margin, the so-called Mentawai segment remained unbroken in the past five years and Padang city lies in front of on this segment.

Japan Meteorological Agency (JMA) issues the tsunami warnings/advisories based on hypocentral parameters such as the location, depth and magnitude, and a tsunami simulation database system which stores more than hundred thousand cases of previously conducted tsunami simulation results. JMA also monitors the changing of sea level data observed at of 172 tide gauges and 12 GPS buoys located about 10 to 20 km off the coast. By using the tsunami wave observation data of the GPS buoys, JMA estimated the tsunami heights at the coast deduced from the offshore data. For the 2011 Tohoku earthquake (Ozaki, 2011) JMA classifies the tsunami forecast into two cirteria, tsunami warning and tsunami advisory.

The purpose of this study is to estimate the arrival time and the height of tsunami waves which will be observed at OBTM or GPS buoy by adopting the proposed models of historical earthquakes. For an improvement of the coastal tsunami forecast, we tried to evaluate them by making

*Indonesian Agency for Meteorology, Climatology and Geophysics (BMKG), Jakarta, Indonesia.
**International Institute of Seismology and Earthquake Engineering (IISEE), BRI, Tsukuba, Japan.

discussion about the effectiveness of the current location of the offshore tsunami sensors in relation to detect the tsunami before arriving at coastal area of Padang city.

2. THEORY AND METHODOLOGY

2.1 Methodology for near-field tsunami forecast

2.1.1 Basic equations

A non linear long wave approximation for the equation of motion, and equations of continuity with bottom friction without Coriolis force (Satake, 1995), are needed in order to estimate tsunami height at the offshore output points using a numerical simulation. The equations are below :

$$\frac{\partial Vx}{\partial t} + V_x \frac{\partial Vx}{\partial x} + V_y \frac{\partial Vx}{\partial y} = -g \frac{\partial h}{\partial x} - C_f \frac{Vx\sqrt{Vx^2 + Vy^2}}{d + h} \quad (1)$$

$$\frac{\partial Vy}{\partial t} + V_x \frac{\partial Vy}{\partial x} + V_y \frac{\partial Vy}{\partial y} = -g \frac{\partial h}{\partial y} - C_f \frac{Vy\sqrt{Vx^2 + Vy^2}}{d + h} \quad (2)$$

$$\frac{\partial h}{\partial t} + \frac{\partial V_x}{\partial x}\{V_x(h + d)\} + \frac{\partial}{\partial y}\{V_x(h + d)\} = 0$$

,where Vx and Vy are the average velocity in the directions of x (east) and y (south) components, respectively. h is sea surface displacement, d is sea depth, C_f is bottom friction coefficient and g is gravity acceleration (9.8 m/s^2).

2.1.2 Numerical simulation

The tsunami propagation and wave height distributions at output points are calculated by using TUNAMI-N2 code based on uniform grid systems in Cartesian coordinate with a single domain of computation area. Meanwhile, TUNAMI-F1 is used to calculate Green's functions at offshore output points (GPS Bouy/OBTMs) and coastal output points (OPs) for all subfaults and to estimate the tsunami height for each output point. An initial sea-surface displacement model is needed for the computation of Green's functions. The slip amount on the subfault is related directly with the crustal deformation. Hence, the tsunami height/amplitude is also linearly related to the slip amount. The tsunami amplitude for different slip can be estimated once the tsunami waveform for a certain amount of slip is computed (Satake, 1995). The observed tsunami waveform is expressed as a linear superposition of Green's functions as follows :

$$A_{ij}(t)X_j = b_i(t) \quad (3)$$

$A_{ij}(t)$: Green's function/computed waveform at the *i*th station from the *j*th subfault
X_j : Slip amount on the *j*th subfault
$b_i(t)$: Observed tsunami waveform at the *i*th station

The dimensions of the computation area are set to 540 grid points for longitude and 540 grid points for latitude in the region between 94°E-103°E in longitude and 1°N-8°S in latitude. In a wave equation, the CFL (Courant Friedrics Lewy) condition should be satisfied for stability of numerical computation given by the following formula (Imamura et al., 2006):

$$\Delta t \le \frac{\Delta x}{\sqrt{2gh_{max}}} \quad (4)$$

,where Δt and Δx are the temporal and spatial grid lengths, and h_{max} is the maximum still water depth in a computation region. In order to stabilize the numerical computation, the temporal grid sizes (Δt) were set to 3.0 s for a uniform grid of 1 arc-minute bathymetry data computations and 2.0 s for a uniform grid of 30 arc-second bathymetry data.

3. DATA

3.1 Ocean bottom tsunami meters (OBTMs) and GPS buoy

There is an OBTM observation system located around Mentawai islands and the off coast West Sumatra, which is operated by BPPT. Within the stations, three GPS buoy systems along the

Sunda trench subduction zone are covered in this study (Table 1). The OBTM and GPS buoy data are recorded and transmitted in real-time to the Real-time Data Server (RDS) at BPPT office.

Table 1. Location of output points and water depth in bathymetry data from GEBCO

No	Code	Location	Lat.	Lon.	Depth (30 Arc-Second)	Type	Remarks
1	TM1	North East Sipora island	-1:56	100:02	1714	OBTM	Active
2	TM2	South West Sipora island	-2:47	98:54	5579	GPS Buoy	No data to RDS
3	TM3	South West Sipora island	-0:35	97:23	5348	GPS Buoy	No data to RDS
4	TM4	South of Pagai island	-4:58	100:33	6173	GPS Buoy	No data to RDS
5	OP1	Pariaman city	-0:37	100:06	3	Tide Gauge	Assumed
6	OP2	Padang city	-0:57	100:20	11	Tide Gauge	Assumed
7	OP3	Bayang city	-1:18	100:29	24	Tide Gauge	Assumed
8	OP4	Jurai city	-1:21	100:33	14	Tide Gauge	Assumed
9	OP5	Sutera city	-1:35	100:38	29	Tide Gauge	Assumed
10	OP6	Lengayang city	-1:41	100:41	33	Tide Gauge	Assumed

3.2 Scenario earthquakes

We adopt three scenarios (Natawidjaja et al., 2006) of tsunamigenic earthquakes for tsunami simulation. These scenarios consist of multisegments with different slip models, referring to the source parameters of the 1797 and 1833 Sumatra earthquakes (Table 2). For all scenarios, we consider different sizes and slip of each segment as shown in Table 3. The top depth of the fault for scenario 1 is set to be 5000 m and for scenarios 2 set to be 1000 m while for scenario 3 set to be zero since the fault planes are located near the trench. We used bathymetry data from the General Bathymetric Chart of the Ocean (GEBCO) with 1 arc-minute and 30 arc-second resolution. We tried to obtain and compare the synthetic result of the tsunami heights at the OBTMs and buoys using modeling codes called TUNAMI-N2 and TUNAMI-F1.

Table 2. Fault parameters for all scenarios

No	Scenario	Mw (yr)	Segment	Length (km)	Width (km)	Strike (°)	Dip (°)	Rake (°)	Slip (°)	Top Depth (m)	Latitude (°)	Longitude (°)
1	1	8.6 (1833)	A	180.55	79.01	325	10	100	10	5000	-4.42	100.9
2			B	70	116.17	325	10	100	9	5000	-3.083	99.97
3			C	26.73	88.83	325	10	100	7	5000	-2.561	99.6050
4	2	8.7 (1797)	A	18.13	147.58	325	10	100	4	1000	-3.66	99.62
5			B	67.42	139.44	325	10	100	6	1000	-3.528	99.525
6			C	75.19	130.11	325	10	100	8	1000	-3.03	99.17
7			D	212.78	147	325	10	100	6	1000	-2.47	98.785
8	3	8.9 (1833)	A	165	135	325	10	100	18	0	-4.70	100.38
9			B	71.66	180	325	10	100	11	0	-3.47	99.52
10			C	31.30	180	325	10	100	9	0	-2.94	99.15

4. RESULTS AND DISCUSSION

4.1 Seafloor deformation for all scenarios

The initial conditions for all scenarios are calculated based on the input parameters in Table 2. Referring to research conducted by Natawidjaja et al. (2006), there are three segments with different slip values for scenario 1 (Figure 1a) and four different segments for scenario 2 (Figure 1b), and three segments for scenario 3 (Figure 1c). Along the cross section from 98°E to 101.5°E, the uplift and subsidence are ranging from 5 m to -4 m depend on the slip amount of each scenario. For scenario 1, we obtained the maximum subsidence of 2 m and the uplift of 3 m. For scenario 2, the top edge depth of this fault is set to be zero which makes the fault area is close to the trench. The size of the fault in scenario 2 is about 370 km x 577 km which covers almost all the area of the Mentawai islands, from south Hibala island in the north until the southern part of South Pagai island. The maximum subsidence obtained for scenario 2 was 1.6 m and 1.4 m for the uplift. For scenario 2, 1 offshore output point (TM1) and 6 coastal output points are located in subsidence area. For scenario 3, The fault area has slip varying between 9 and 18 m. The size of the fault plane is approximately 267 km in width and 495 km in length. The maximum subsidence of 3.6 m and the uplift of 3.2 m are estimated in this scenario.

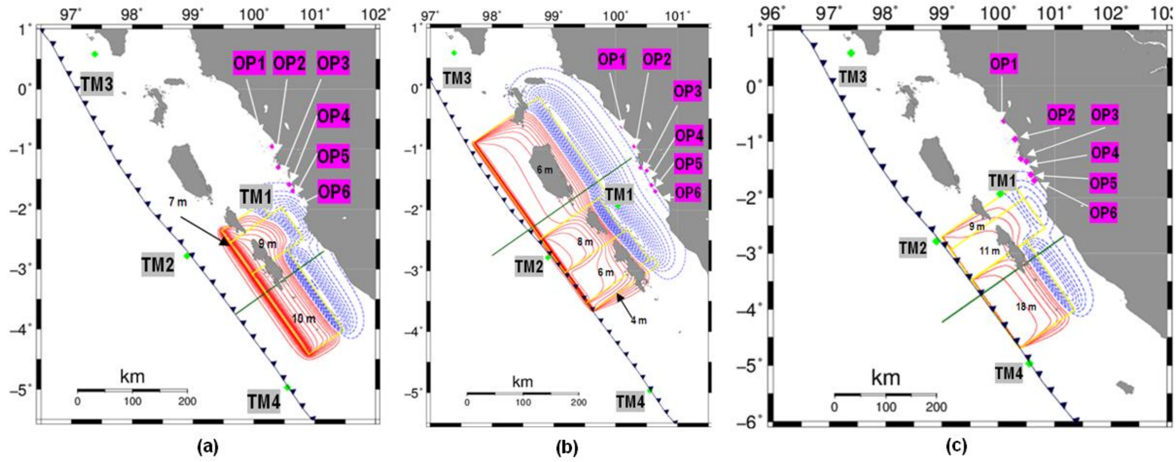

Figure 1. (a) Seafloor deformation for scenario 1. Blue dash lines and red lines show the subsidence and uplift area respectively. The contour intervals are 0.2 m. Green diamonds show the location of the offshore tsunami meters while pink diamonds are the coastal output points. The thick green line shows the cross section (b) Seafloor deformation for scenario 2. the contour intervals are 0.1 m. (c) Seafloor deformation for scenario 3. The contour intervals are 0.5 m.

4.2 Maximum tsunami height

Maximum tsunami heights for scenario 2 were obtained from the west coast area of Mentawai island, Sipora island to the west coast of North Pagai island (Figure 2b), while the maximum tsunami heights for scenario 1(Figure 2a) were obtained at the southwest area of Sipora island to the south of Pagai island ocean side. From Figure 2b, we can identify that the most of tsunami energy are heading to the Indian ocean. The pattern of the maximum tsunami height for scenario 3 (Figure 2c) is almost similar to other scenarios. However, for scenario 3, the maximum tsunami height involves much wider area, this could be due to the large amount of slip distribution.

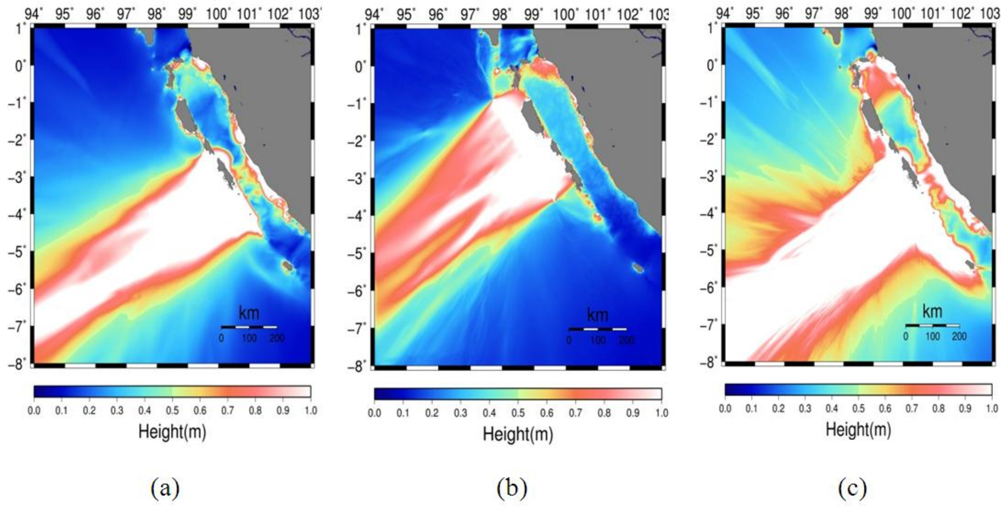

Figure 2. Estimated maximum tsunami height for (a) scenario 1, (b) scenario 2 and (c) scenario 3. Based on the scale, dark color shows lower tsunami height while brighter color shows higher tsunami waves.

4.3 Comparison of the initial tsunami height for scenario 2

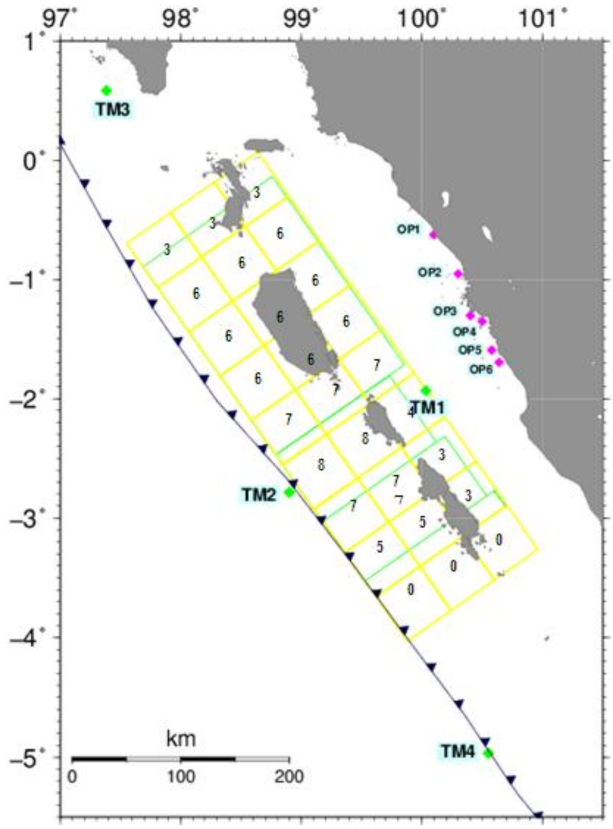

In this study, scenario 2 was selected as the scenario representing the unbroken segment. To calculate Green's function in for all output points we made 27 subfaults with the fault size of 50 km x 50 km and slip of 1 m covering the scenario fault area (Figure 3). We also compare the scenario 2 results obtained by using different source codes (TUNAMI-N2 and TUNAMI-F1) using the 1 arc-minute bathymetry data. A numerical simulation to obtain tsunami waveforms was performed using the output points data in Table 2. To find the relationship between offshore output points (TM1-TM4) and coastal output points (OP1-OP6), we compare the arrival time and the initial height of tsunami waveform. Using TUNAMI-F1 code for the bathymetry data of 1 arc-minute, the calculated tsunami height at OP2 (Padang city) are in the range of 3-4 m. At most of the offshore output points (TMs) the first positive waveforms arrived in less than 13 min (Table 3).

Figure 3. Subfault model for scenario 2. The green rectangles shows the different sizes of fault segments for scenario 2 with slip varying between 4 and 8 m. Yellow boxes within the fault areas show the assumed subfaults with 50 km x 50 km size and 1 m slip for each. The number within every subfault is a slip amount. The green diamonds are the locations of the offshore tsunami meters while pink diamonds are the coastal output points.

Table 3. Arrival times and heights of initial tsunami waveform

Bathymetry 1 Arc-Minute					Bathymetry 30 Arc-Second	
Stations	TUNAMI-N2		TUNAMI-F1		TUNAMI-N2	
	Time (min)	Heights (m)	Time (min)	Heights (m)	Time (min)	Heights (m)
TM1	6.3	-0.114	6.7	-0.0027	6.3	-0.145
TM2	0.9	0.404	0.8	1.48	0.8	1.547
TM3	4.2	0.139	1.9	0.0347	3.9	0.109
TM4	13	0.078	12.8	0.0279	12.6	0.068
OP1	37.5	0.782	39.3	2.7482	33.1	1.791
OP2	35.5	0.277	36.8	0.2914	35.3	-0.168
OP3	67.5	0.229	52.3	0.0432	60.7	0.197
OP4	78.2	0.199	67.4	0.183	61.6	0.037
OP5	63.8	0.709	60.2	0.269	65.4	0.423
OP6	55.6	0.078	53.1	0.1723	49.3	-0.1

4.4 Tsunami travel time to coastal points

We estimated the initial tsunami arrival time within the range 0.8-12.8 min at the offshore output points (TM1-TM4) by using TUNAMI-N2 with 1 arc-minute bathymetry data. Based on tsunami arrival time data at TM4, It took about 35 min before the tsunami wave reachs OP2 which is the coastal output point of Padang city. As comparison, we also calculated the initial tsunami arrival time using TUNAMI-F1 with 1 arc-minute bathymetry data. The earliest arrival time was 0.8 min at TM2 offshore output point. We found that the initial tsunami arrival time for the offshore output point (TM1-TM4) are not so much different if we compare the result obtained by using TUNAMI-N2 and TUNAMI-F1. Moreover, the computation using the 30 arc-second grid produces relatively faster arrival time of tsunami. This might be caused by the accuracy of bathymetry data.

4.5 Real-time tsunami forecast

The concept of a real-time tsunami forecast in this study is based on a high precision of the initial tsunami height at nearby coastal output points (OP1-OP6) when the offshore output points (TM1-TM4) detect a change of the sea level as the initial tsunami height on real time. The difficulties to issue tsunami forecasting occur when the epicenter of the earthquakes is close to the target area. Therefore, this problem might be solved if we can introduce information about the tsunami source into the forecasting scheme by conducting a tsunami waveform inversion for slip distribution on an assumed fault plane (Tsushima et al., 2009). The other way to overcame the problem of inaccurate tsunami forecasts is to increase the density of OBTM stations with appropriate spatial distribution.

5. CONCLUSIONS

In this study, we made a simple forecasting of tsunami height and also estimated the arrival times of tsunami waves in the coastal area of Padang city, using the 1797 and 1833 earthquakes that took place in the west coast of Sumatra island. We chose the 1797 earthquake (scenario 2) since it fulfills the criteria of a tsunamigenic earthquake and the epicenter is located in the unbroken segment for the past 200 year. Using scenario 2, we compared all the results with different bathymetry data and found that the differences of initial tsunami arrival time for the offshore output points (TM1-TM4) are not so significant. Contrarily, based on the numerical simulation with the finer resolution of bathymetry data, we obtained faster initial tsunami arrival times at the most of coastal output points.

The accuracy of coastal tsunami height can be affected by a spatial relationship between the tsunami source and OBTMs. Considering the effect of the radiation pattern from the tsunami source, an unaccuracy of tsunami forecasting would be reduced by deploying more OBTMs at the offshore of Padang.

REFERENCES

Imamura, et al., 2006, Tsunami Modelling Manual (TUNAMI model), DCRC (Disaster Control Research Center, Tohoku University, Sendai, Japan.

Natawidjaja, et al., 2006, Journal of Geophysical Research, Vol. 111, B06403, doi:10.1029/2005JB004025.

Ozaki T, 2011, Outline of the 2011 off the Pacific coast of Tohoku earthquake (Mw 9.0) – Tsunami warnings/advisories and observations, Earth Planet Space.

Satake, K., 1995, PAGEOPH, 144, 455-470

Tsushima, et al., 2009, Vol. 114, B06309, doi:10.1029/2008JB005988, 2009.

Website : General Bathymetric Chart of the Ocean (GEBCO) http://www.bodc.ac.uk/data/online_delivery/gebco/.